

Numerical Study of Turbulent Flow over Backward-Facing Step with Different Turbulence Models

D. G. Jehad^{*,a}, G. A. Hashim^b, A. K. Zarzoor^c and C. S. Nor Azwadi^d

Department of Thermo-Fluids, Faculty of Mechanical, Engineering, Universiti Teknologi Malaysia, 8310 Skudai, Johor Bahru, Malaysia

^{a,*} dhafir_alalwan@yahoo.com, ^bghasaq_88@yahoo.com, ^cahmedmechano1@gmail.com, ^dazwadi@fkm.utm.my

Abstract – Numerical studies are conducted on turbulent incompressible flow over 2D backward-facing step in order to investigate the performance of three different turbulence models (standard k - ϵ , realizable k - ϵ and SST k - ω) in predicting the region of separation and reattachment behind the edge of step. Current solutions of Reynolds number ($Re = 13200$) and expansion ratio ($H: H_2 = 1:3$) are compared with experimental measurements. Among the turbulence models, SST k - ω and standard k - ϵ exhibited good agreement with experimental results. **Copyright** © 2015 Penerbit Akademia Baru - All rights reserved.

Keywords: Turbulence model; Turbulent flow; Backward-facing step; Separation; Reattachment

1.0 INTRODUCTION

Flow over a backward-facing step is accounted as a major reason by which recirculation zones are generated and vortices are formed because of the separation flow obtained from the counter pressure gradients in the flow of fluid [4]. The fluid flow over a backward-facing step has become a significant essential subject by which the separation and reattachment processes of turbulent shear layers can be investigated in various practical engineering applications such as internal flow systems (e.g. combustors, diffusers) and flow over airfoils and buildings [1-2]. The two-dimensional (2-D) backward-facing step gives a superior state for investigating the fundamental physical phenomena of separation and reattachment due to its geometrical simplicity [3]. This flow is also considered an important test which can be employed in order to compare between the turbulence models. With the redundancy of data in literature, the flow over a backward facing step is frequently employed as a case of benchmark test for several CFD codes and models related to turbulent flow. A variety of turbulence models such as RANS, LES and DNS have all been employed in order to simulate this flow in 2D domain and 3D as well [5].

Armaly et al. [3], they studied a backward-facing step flows experimentally and numerically. They noticed a variance in the results of length of major recirculation which obtained from the experimental and the numerical work. In addition, they observed a region of secondary flow at the upper wall of channel. Eaton and Johnston [6] investigated the separation of flow back a rearward facing step experimentally. A vortex module was noticed in the layer of free shear as the separating boundary layer was turbulent. Lee and Mateescu [8] conducted an

experimental and numerical study of flow of air over a two-dimensional backward-facing step. They noticed a good agreement between the numerical and experimental results in terms of the position of the separation and reattachment points. Le et al. [9] studied turbulent flows past a backward-facing step numerically. The immediate velocity domain appeared the change of reattachment length in the spanwise direction and also the flow showed a robust structure of streamwise vortex. Sinha et al. [7] conducted the turbulent region past backward-facing step. They noticed that for Re higher than 10000, the region of re-attachment almost becomes a fixed value step height. Adams and Johnston [10] investigated flow over a backward facing step experimentally. They found that the length of reattachment for the case of turbulent boundary layers upstream of the step was higher compared to the laminar upstream boundary layers. Scarano and Reithmuller [32] investigated the recirculation region characteristics behind backward-facing step. They found that the main vortex stretch from the edge of step to the point of reattachment whereas the counter-rotating secondary vortex remains in the corner of the step wall. However in the present work, the main goal is to analyze and compare the separation and reattachment regions of flow over 2D backward-facing step based on three different turbulent models (standard $k-\mathcal{E}$, realizable $k-\mathcal{E}$ and SST $k-\omega$)

2.0 MATHEMATICAL MODELLING

2.1 Problem definition

A schematic view of 2D backward facing step is shown in Fig. 1. [13]. the flow entering from the left side dissociates at the sharp corner of the step after that reattaches again to the lower wall at a distance L, behind the step. A recirculation region is subsequently produced directly behind the step. The expansion ratio which represents the step height (H) to outlet channel height (H₂) is 1:3 and the Reynolds number is 13200.

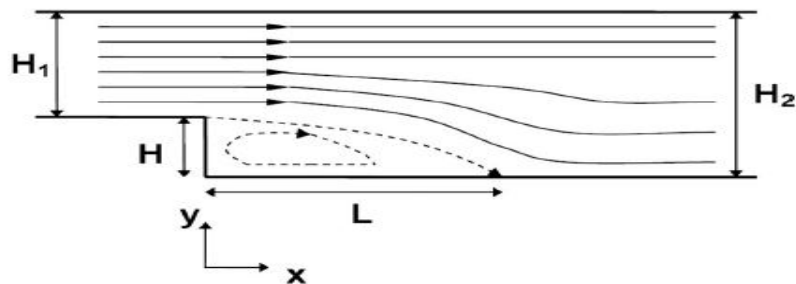


Figure 1: Geometry and flow style of the backward-facing step

2.2 Governing equations

The equations of conservation of mass and momentum in the case of incompressible and stationary turbulence can be written in Cartesian-tensor notation as

$$\frac{\partial U_i}{\partial x_i} = 0 \quad (1)$$

$$U_j \frac{\partial U_i}{\partial x_j} = -\frac{1}{\rho} \frac{\partial p}{\partial x_i} + \frac{\partial}{\partial x_j} \left(\nu \left(\frac{\partial U_i}{\partial x_j} + \frac{\partial U_j}{\partial x_i} \right) - \overline{u'_i u'_j} \right) \quad (2)$$

The term $\overline{u'_i u'_j}$ which is known as the Reynolds-stress tensor, has to be determined with a turbulence models.

2.3 Turbulence modelling

Different turbulent models can be employed to compute a solution of the governing equations, in this work in order to analyse turbulent flow over 2D backward facing step in terms of the separation and reattachment, three turbulent models (standard k-ε, realizable k-ε and SST k-ω) are implemented.

2.3.1 The standard k-ε model

The correlations of this model are [11]:

$$U_i \frac{\partial k}{\partial x_i} - \frac{\partial}{\partial x_i} \left[\frac{\nu_T}{\sigma_k} \frac{\partial k}{\partial x_i} \right] = P - \varepsilon, \quad (3)$$

$$U_j \frac{\partial \varepsilon}{\partial x_j} - \frac{\partial}{\partial x_i} \left[\frac{\nu_T}{\sigma_\varepsilon} \frac{\partial \varepsilon}{\partial x_i} \right] = \frac{\varepsilon}{k} (C_{\varepsilon 1} P - C_{\varepsilon 2} \varepsilon), \quad (4)$$

$$\nu_T = C_\mu \frac{k^2}{\varepsilon}, \quad (5)$$

$$P_k = -\overline{u'_i u'_j} \left(\frac{\partial U_j}{\partial x_i} + \frac{\partial U_i}{\partial x_j} \right), \quad (6)$$

$$\overline{u'_i u'_j} = \frac{2}{3} \delta_{ij} k - \nu_T \left(\frac{\partial U_j}{\partial x_i} + \frac{\partial U_i}{\partial x_j} \right) \quad (7)$$

where $C_\mu=0.09$, $C_{\varepsilon 1}=1.44$, $C_{\varepsilon 2}=1.92$, $\sigma_k = 1$ and $\sigma_\varepsilon = 1.3$ are the constants of the model and P_k signifies the production rate of the turbulence kinetic energy. ν_T is the Boussinesq eddy viscosity, while the turbulence Reynolds stress tensor is calculated with the help of the generalized Boussinesq hypothesis (Eq. (5)).

2.3.2 The realizable k-ε model (RKE)

The k equation is identical with the standard k-ε and ε equation is given by

$$\frac{\partial U_j \varepsilon}{\partial x_j} = \left(\mu + \frac{\mu_t}{\sigma_\varepsilon} \right) \nabla^2 \varepsilon + C_1 S \rho \varepsilon - C_2 \frac{\rho \varepsilon^2}{k + \sqrt{\nu \varepsilon}}, \quad (8)$$

where $C_1 = \max[0.43, \eta/(\eta+5)]$, $C_2 = 1.0$, $\sigma_k = 1.0$, $\sigma_\varepsilon = 1.2$

$\eta = Sk/\varepsilon$, η : represents is the ratio between the time scales of the turbulence and the mean flow.

$S = \sqrt{2S_{ij}S_{ij}}$, S denotes the mean strain-rate of the flow S_{ij} the deformation tensor.

2.3.3 The SST (shear stress transport) k-ω Turbulence Model

The formulation of SST k-ω is given by [12] as follow

Turbulent kinetic energy:

$$U_i \frac{\partial k}{\partial x_i} = P_k - k\omega\check{\beta} + \frac{\partial}{\partial x_i} \left[(\mu + \sigma_k \mu_t) \frac{\partial k}{\partial x_i} \right] \quad (9)$$

Specific dissipation rate:

$$U_i \frac{\partial \omega}{\partial x_i} = \alpha S^2 - \beta \omega^2 + \frac{\partial}{\partial x_i} \left[(\mu + \sigma_{\omega 1} \mu_t) \frac{\partial \omega}{\partial x_i} \right] + 2(1 - F_1) \sigma_{\omega 2} \frac{1}{\omega} \frac{\partial k}{\partial x_i} \frac{\partial \omega}{\partial x_i} \quad (10)$$

Where F_1 is the blending function given by

$$F_1 = \tanh \left\{ \left\{ \min \left[\max \left(\frac{\sqrt{k}}{\beta \omega y}, \frac{500\nu}{y^2 \omega} \right), \frac{4\rho \sigma_{\omega 2} k}{CD_{k\omega} y^2} \right] \right\}^4 \right\} \quad (11)$$

$$CD_{k\omega} = \max \left(2\rho \sigma_{\omega 2} \frac{1}{\omega} \frac{\partial k}{\partial x_i} \frac{\partial \omega}{\partial x_i}, 10^{-10} \right) \quad (12)$$

y is the distance to the nearest wall.

The turbulent eddy viscosity for the SST model is defined as follows

$$\mu_t = \frac{a_1 k}{\max(a_1 \omega, SF_2)} \quad (13)$$

Where S is the vorticity magnitude, and the blending function F_2 can be obtained from:

$$F_2 = \tanh \left[\left[\max \left(\frac{2\sqrt{k}}{\beta \omega y}, \frac{500\nu}{y^2 \omega} \right) \right]^2 \right] \quad (14)$$

$$y_1 = \frac{\beta_1}{\check{\beta}} - \frac{\sigma_{\omega 1} \lambda^2}{\sqrt{\check{\beta}}}, y_2 = \frac{\beta_2}{\check{\beta}} - \frac{\sigma_{\omega 2} \lambda^2}{\sqrt{\check{\beta}}} \quad (15)$$

The constants are taken from the ref. [12]:

$$\check{\beta} = 0.09, a_1 = 0.31, \lambda = 0.41$$

$$\beta_1 = 0.075, \sigma_{\omega 1} = 0.5, \sigma_{k1} = 0.85$$

$$\beta_2 = 0.0828, \sigma_{\omega 2} = 0.856, \sigma_{k2} = 1.0$$

3.0 NUMERICAL APPROACH

The computational solution is implemented by employing the commercial pre-processor software FLUENT 14.0 which is also employed for making the mesh, boundary conditions setting and then the finite volume method is used to discretize the governing equations. SIMPLE algorithm is used to solve the velocity-pressure coupled equation. The convergence criterion was set to 10^{-6} in order to achieve more accurate convergence.

4.0 RESULTS AND DISCUSSION

This part introduces a comparison between the simulations results with the three different turbulence models which are the standard k- ϵ , the realizable k- ϵ and the SST k- ω . The goal of this work is not only to validate the CFD model but also to compare the performance of the different turbulence models in terms of mean streamlines and the mean velocity profiles.

4.1 Grid optimization and validation

To confirm the validity and accuracy of the numerical work, for this purpose three grid densities have been experienced with standard k- ϵ , which are 150 by 85 and 205 by 105 and 250 by 105 So in terms of saving time and accuracy, it is found that the system with grid density 205 by 105 can be adopted in this computation as shown in figure (2) In order to proof the validation and precision of the numerical work, the mean velocity profile compared with experimental work of of Kim [13]. It can be shown from Figure (2), there is a very good agreement between the computed and experimental results, and the deviation is around 5%.

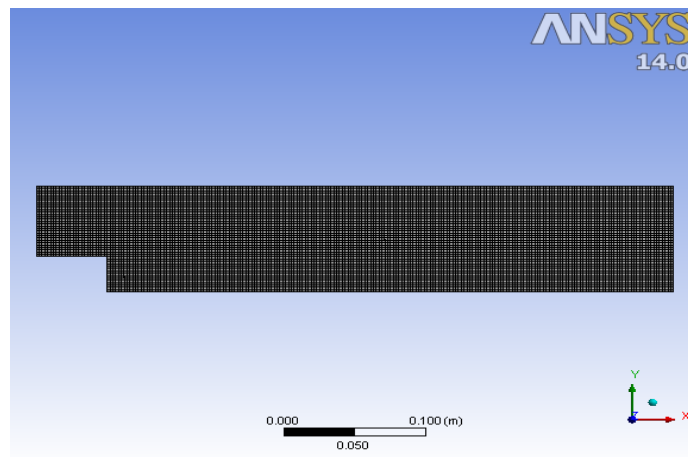


Figure 2: Grid optimization

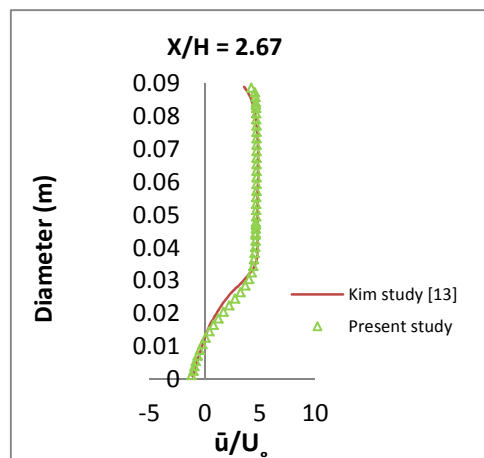


Figure 3: Validation of Computed mean velocity profile with experimental work at selected location

4.2 Comparison of turbulence models

The computed results obtained for turbulent flow over a backward-facing step for Reynolds number $Re = 132,000$ and an expansion ratio of 1: 3 with three turbulence models (standard $k-\epsilon$, realizable $k-\epsilon$ and SST $k-\omega$).

4.2.1 Reattachment length

The computed streamlines obtained from the standard $k-\epsilon$, realizable $k-\epsilon$ and SST $k-\omega$ models are shown in Fig. 4. It can be seen that they all have similar behaviour in terms of separation but there is a difference in the length of reattachment length. SST $k-\omega$ clearly indicates a longer reattachment length of $L/H = 7.2$ compared to the reattachment points of both standard $k-\epsilon$ and realizable $k-\epsilon$ which are 6 and 6.7, respectively. On the other hand, according to Kim [13], the reattachment point was around $L/H=7.1$. It is noticed that SST turbulence model results provide a good agreement with the experimental work, which might occur due to its high performance to predict a greater degree of turbulence kinetic energy compared to other models.

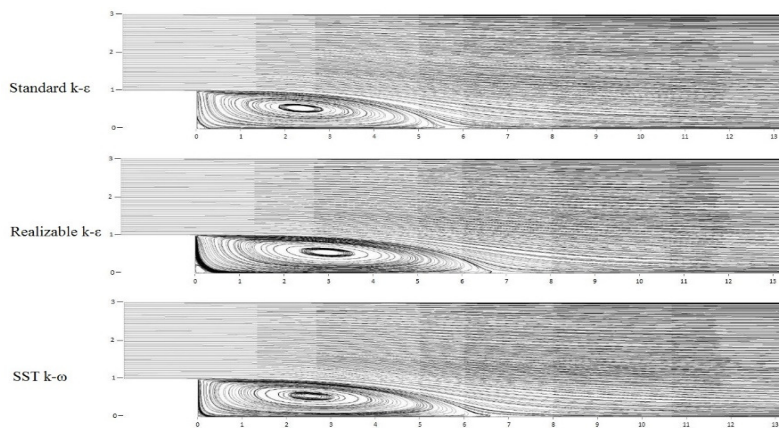


Figure 4: Computed results of streamline for three turbulent models

4.2.2 Mean velocity profile

The all three turbulent models exhibited recirculation regions at different locations behind the step, this attitude can be represented at high velocity gradient as shown in figure (5a, 5b, 5c, 5d, 5e, 5f) of mean velocity profile. This behaviour arises from the adverse pressure gradient at the edge of the step due to separation of boundary layers and high turbulent movement. Also it is seen that the velocities are almost zero near to the walls because of the highest shear stress. However, from the results of velocity profile figure 5, it can be shown that standard $k-\epsilon$ model results is closer to the obtained results of velocity profile of experimental work compared to other models at different locations on x-axis behind the step.

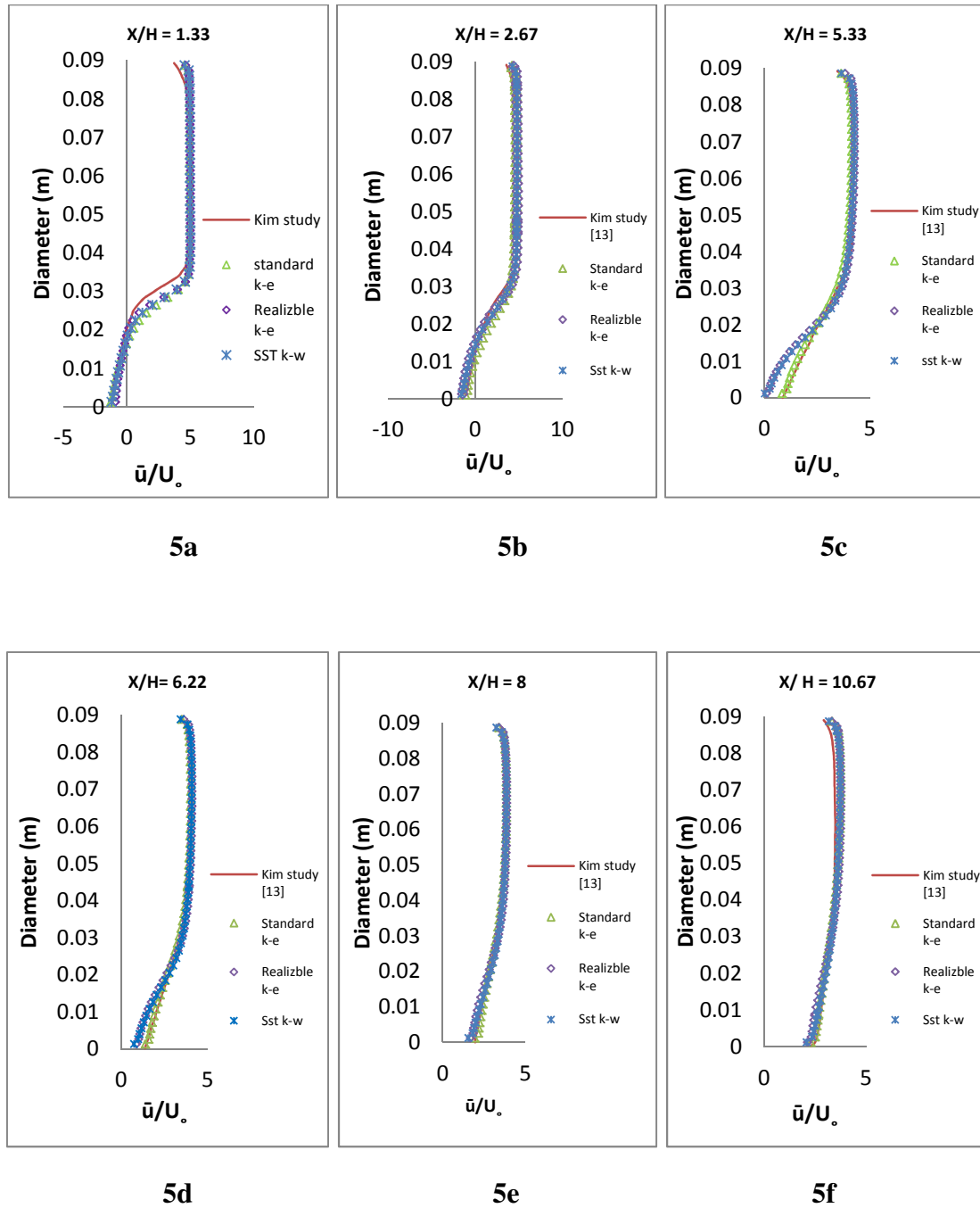


Figure 5: comparison of computed mean velocity profiles for three turbulence models with experimental data

4.0 CONCLUSION

In this work, numerical study of turbulent flow over backward-facing step has been implemented with three turbulence models (standard k- ϵ , realizable k- ϵ and SST k- ω).the SST k- ω model showed very good agreement with experimental data in terms of the length of reattachment region whereas the standard k- ϵ model exhibited satisfactory results in terms of mean velocity profile to the experimental data.

REFERENCES

- [1] W.C. Lasher, D.B. Taulbee, On the computation of turbulent backstep flow, *International Journal of Heat and Fluid Flow* 13 (1992) 30-40.
- [2] H. Le, P. Moin, J. Kim, Direct numerical simulation of turbulent flow over a backward-facing step, *Journal of Fluid Mechanics* 330 (1997) 349-374.
- [3] B.F. Armaly, F. Durst, J.C.F. Pereira, B. Schönung, Experimental and theoretical investigation of backward-facing step flow, *Journal of Fluid Mechanics* 127 (1983), 473-496
- [4] H. Togun, M.R. Safaei, R. Sadri, S.N. Kazi, A. Badarudin, K. Hooman, E. Sadeghinezhad, Numerical simulation of laminar to turbulent nanofluid flow and heat transfer over a backward-facing step, *Applied Mathematics and Computation* 239 (2014) 153-170.
- [5] M. Shahi, M. J.B. Kok, A. Pozarlik, On characteristics of a non-reacting and a reacting turbulent flow over a backward facing step (BFS), *International Communication in Heat and Mass Transfer* (2014) 16-25.
- [6] J.K. Eaton, J. P. Johnston, (1980). Turbulent flow reattachment: an experimental study of the flow and structure behind a backward-facing step, Stanford University.
- [7] S.N. Sinha, A.K. Gupta, M. Oberai, Laminar separating flow over backsteps and cavities. I-Backsteps, *AIAA Journal*, 19 (1981), 1527-1530.
- [8] T. Lee, D. Mateescu, Experimental and numerical investigation of 2D backward-facing step flow, *Journal of Fluids and Structures* 12(1998) 703-716.
- [9] H. Le, P. Moin, J. Kim, Direct numerical simulation of turbulent flow over a backward-facing step, *Journal of Fluid Mechanics* 330 (1997) 349-374
- [10] E.W. Adams, J.P. Johnston, Effects of the separating shear layer on the reattachment flow structure Part 2: Reattachment length and wall shear stress, *Experiments in Fluids* 6, (1988) 493-499.
- [11] B.E. Launder, D.B. Spalding, The numerical computation of turbulent flows, *Computer Methods in Applied Mechanics and Engineering* 3 (1974), 269-289.
- [12] F.R. Menter, Two-equation eddy-viscosity turbulence models for engineering applications, *AIAA Journal* 32 (1994), 1598-1605
- [13] J. Kim, S.J. Kline, J.P. Johnston, Investigation of a reattaching turbulent shear layer: flow over a backward-facing step, *Journal of Fluids Engineering* 102 (1980) 302-308.
- [14] F. Scarano, M. L. Reithmuller, Iterative multigrid approach in pv image processing with discrete window offset, *Experiments in Fluids* 26 (1999) 513-523.